Intermetallics 43 (2013) 24–28

Contents lists available at ScienceDirect

Intermetallics

journal homepage: www.elsevier.com/locate/intermet

Effect of strain rate on the compression behavior of TiAl and TiAl–2Mn alloys fabricated by combustion synthesis and hot press consolidation

Shili Shu, Feng Qiu, Bin Xing, Shenbao Jin, Jinguo Wang*, Qichuan Jiang*

Key Laboratory of Automobile Materials, Ministry of Education, and Department of Materials Science and Engineering, Jilin University, No. 5988 Renmin Street, Changchun 130025, People's Republic of China

ARTICLE INFO

Article history:
Received 2 March 2012
Received in revised form
23 June 2013
Accepted 8 July 2013
Available online 31 July 2013

Keywords:
A. Titanium aluminides, based on TiAl
B. Work-hardening
C. Reaction synthesis
F. Mechanical testing

ABSTRACT

Compression tests of the TiAl and TiAl–2Mn alloys have been performed in the strain rate range from 1×10^{-5} s^{-1} to 1×10^{-2} s^{-1}, and the effect of strain rate on the compression properties and work-hardening behavior of the two alloys have been investigated. Under any strain rate, the ultimate compression strength (σ^{UCS}_{true}) and the fracture strain (ε^{f}_{true}) of the TiAl–2Mn alloy are better than those of the TiAl alloy, while the work-hardening capacity (H_c) of the TiAl–2Mn alloy is lower than that of the TiAl alloy. The yield strength (σ^{y}_{true}) and H_c of the two alloys are strain rate sensitive, while the σ^{UCS}_{true} and ε^{f}_{true} are insensitive to the strain rate. With the increase in the strain rate, the σ^{y}_{true} increases, while the H_c decreases.

1. Introduction

TiAl-based alloys (γ-TiAl + α_2-Ti_3Al) have great potential as high temperature structural materials due to their low density, high melting point, good creep characteristic and excellent oxidation/corrosion resistance [1–3]. For structural components, the reliable design is of utmost importance and it requires an understanding of their mechanical properties under different loading conditions.

In the past several decades, the effect of strain rate on the deformation behavior of TiAl alloys has attracted continuous attention and was reported [4–7]. Pu et al. reported that the compression strength of TiAl–Cr–V alloy will increase at 1170 °C when the strain rate changes from 10^{-3} to 10^{0} s^{-1} [4]. Liu et al. also reported that the flow stress of the Ti–45Al–7Nb–0.4W alloy increased with the increase in strain rate (from 10^{-3} s^{-1} to 10^{-1} s^{-1}) when the tests were conducted at the temperature from 1000 °C to 1200 °C [5]. However, these works are mainly focused on the high temperature deformation behavior of TiAl alloys under various strain rates, fewer studies have probed the systematic mechanical behavior of TiAl alloys over a wide range of strain rates at room temperature. It is also important to document the mechanical response of TiAl alloys to strain rates at room temperature in order to ensure the application reliability for TiAl alloys. Moreover, work-hardening behavior is an important factor in the evaluation of the plastic deformation of materials. The deformability, ductility and toughness of materials are intimately linked to the work-hardening capacity [8]. The study on the work-hardening behavior of TiAl alloys, especially the effect of strain rate on it has never been systematic studied.

The TiAl-based alloys reported so far are mostly fabricated by casting approaches [3,9,10]. The new method of combustion synthesis and hot press consolidation takes the advantages of low energy requirement, high purity of the products, low fabrication temperature and the synthesized materials could be used directly [11,12]. Thus, the objective of this paper is to fabricate the TiAl and TiAl–2Mn alloys using the method of combustion synthesis and hot press consolidation and investigate the effect of the strain rate on the compression properties and work-hardening behavior of them at room temperature. Besides, with the purpose of trying to resolve the key problem of low ductility of TiAl alloy, the effect of Mn on the ductility of the TiAl alloy is investigated by the first principle calculation and experiment. It is expected that this study would provide a reference on the practice application and ductility improvement of TiAl alloys under various strain rate conditions.

2. Experimental

The starting materials were made from commercial powders of titanium (99.5% purity, ~25 μm), aluminum (99% purity, ~74 μm)

* Corresponding authors. Tel./fax: +86 431 85094699.
E-mail addresses: jgwang@jlu.edu.cn (J. Wang), jqc@jlu.edu.cn (Q. Jiang).

0966-9795/$ – see front matter © 2013 Elsevier Ltd. All rights reserved.
http://dx.doi.org/10.1016/j.intermet.2013.07.003

and manganese (99.5% purity, ~47 μm). Elemental powder blends corresponding to TiAl and TiAl–2Mn were mixed sufficiently by ball milling for 8 h and then cold pressed into cylindrical compacts using a stainless steel die. The powder compact with 28 mm in diameter and approximately 36 mm in height was contained in a graphite mold, which was put into the self-made vacuum thermal explosion furnace. The heating rate of the furnace was about 30 K/min and the temperature in close to the center of the compact was measured by Ni–Cr/Ni–Si thermocouples. When the temperature measured by the thermocouple suddenly rose rapidly, indicating that the sample should be ignited, the sample was quickly pressed just when it was still hot and soft. The pressure (~50 MPa) was maintained for 10 s and then was cooled down to the ambient temperature.

The phase constituents of the alloys were examined by X-ray diffraction (XRD, Model D/Max 2500PC Rigaku, Japan) with Cu Kα radiation at voltage of 40 kV using a scanning speed of 4°/min. Lattice parameter determinations were obtained using a much slower scanning speed (0.05°/min) performed around the four main peaks of TiAl from 20° to 80°. The microstructure was studied using high-resolution transmission electron microscopy (HRTEM, JEM-2100F, Japan). The cylindrical specimens with a diameter of 3 mm and a height of 6 mm were used for compression tests, and the loading surface was polished to parallel to the other surface. The uniaxial compression tests were carried out under a servo-hydraulic materials testing system (MTS, MTS 810, USA) with constant strain rates of 1×10^{-5} s^{-1}, 1×10^{-4} s^{-1}, 1×10^{-3} s^{-1} and 1×10^{-2} s^{-1}.

The calculation work was performed with the Cambridge Sequential Total Energy Package code (CASTEP) [13]. Brillouin zone was set within $3 \times 3 \times 3$ k point mesh generated by the Monkhorst–Pack scheme [14]. The plane-wave basis cutoff was set as 400 eV for all cases. We have performed more precise testing calculations with a plane-wave cutoff energy of 450 eV, however, the results changed negligibly. Therefore, the value of 400 eV for plane-wave cutoff energy is precise enough for our investigation [15]. According to our previous study and other researchers' work [16–18], the Mn atom prefers the Al site. Thus, in this work, the calculation was performed on the $Ti_{16}Al_{16}$ and $Ti_{16}Al_{15}Mn$ 32-atom supercells.

3. Results and discussion

3.1. Phase identification and microstructure

Fig. 1 shows the XRD patterns for the fabricated TiAl and TiAl–2Mn alloys. The products in the two alloys are mainly γ-TiAl and α_2-Ti_3Al phases. The volume fraction of α_2-Ti_3Al phase in the TiAl and TiAl–2Mn alloys calculated by the method of adiabatic method according to the XRD results are about 16.9 vol.% and 17.6 vol.%, respectively. The Mn element has little effect on the phase composition of the TiAl alloy. As indicated in the insert in Fig. 1, the peak position of the TiAl (111) plane shifts to higher 2θ values with the addition of the Mn element, implying a decrease in the lattice constant of the TiAl. As Mn (0.179 nm) has smaller atomic radius than Al (0.182 nm), the Mn substitution of Al results in the lattice shrink. The SEM image of the TiAl alloy fabricated by the method of combustion synthesis and hot press consolidation has been reported in our previous work [19], and the SEM image of the TiAl–2Mn alloy is similar to that of the TiAl alloy. The TiAl and TiAl–2Mn alloys have similar grain sizes of ~60 μm. The actual concentration of Mn in the TiAl–2Mn alloy detected by energy-dispersive spectra is about 1.36 at.%. According to these results, we believe that the Mn element existed in the TiAl–2Mn alloy is mainly in the form of solid solution.

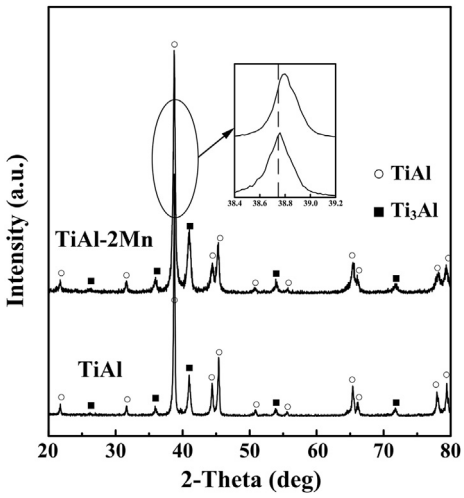

Fig. 1. XRD patterns of the TiAl and TiAl–2Mn alloys.

Fig. 2(a) and (b) shows the TEM images of the TiAl and TiAl–2Mn alloys. It can be seen from Fig. 2(a) that there are a lot of dislocations existed in the TiAl alloy. It indicates that the TiAl alloy fabricated by the method of the combustion synthesis and hot press consolidation possesses higher dislocation density. Fig. 2(b) shows a well developed subgrain structure and a kind of nanometer phase in the TiAl–2Mn alloy. The selected-area electron diffraction (SAED) pattern inserted in Fig. 2(b) obtained from area A corresponds to the $[1\bar{9}6]$ zone axis of the $Al_{19}Mn_4$. According to the HRTEM image of the $Al_{19}Mn_4$ phase, as shown in Fig. 2(c), the synthesized $Al_{19}Mn_4$ phase by the combustion synthesis reaction is in the shape of ellipse and the size is about 15 nm. Fig. 2(d) is the inverse Fourier transformation of the HRTEM image of the area B. The dislocations in TiAl are marked as the "T" shaped symbol. A large number of dislocations exist around the $Al_{19}Mn_4$ phase. It indicates the $Al_{19}Mn_4$ phase would hinder the movement of the dislocations during the following deformation. The dislocation densities in the TiAl and TiAl–2Mn alloys calculated from XRD peak profile analysis [20] are 4.24×10^{12} m^{-2} and 6.52×10^{12} m^{-2}, respectively.

3.2. Compression properties

Fig. 3 shows the compression true stress–strain curves of the TiAl and TiAl–2Mn alloys under different strain rates. The compression properties of the alloys under different strain rates are summarized in Table 1. The σ^{y}_{true} of the two alloys increases with the increase in the strain rate, while there is no significant difference in the σ^{UCS}_{true} and ε^{f}_{true} of the both alloys with the variation in strain rates. Comparing the compression properties of the TiAl and TiAl–2Mn alloys as shown in the insert in Fig. 3, it is observed that TiAl–2Mn alloy shows higher strength and better ductility than the TiAl alloy at any strain rate. At the strain rate of 1×10^{-5} s^{-1}, the σ^{UCS}_{true} of the TiAl–2Mn alloy is 125 MPa higher than that of the TiAl alloy, and the ε^{f}_{true} of the TiAl–2Mn alloy is 18.8% comparing to 17.0% for the TiAl alloy. Because the two alloys have the similar starting microstructures, like grain size and α_2 phase volume fraction, the differences in the compression properties of them could be mainly due to the exist of the nano $Al_{19}Mn_4$ phase, the well developed subgrain structure, the solid solution of Mn and the different contents of dislocation density. The higher strength of the TiAl–2Mn alloy could be mainly due to the hindrance to the slip of dislocations by the nano $Al_{19}Mn_4$ phase, the subgrain boundaries and the stress